above limitations could be met with the present data for either a Venus or Jupiter entry probe mission. Base pressure measurements are also applicable for a Mars probe mission as a means to derive the static freestream pressure profile of the planet. A Mars probe would most likely have a laminar boundary layer during entry; accordingly, Reynolds number effects on base pressure would also have to be considered in addition to the previously mentioned variables for Venus or Jupiter. However, mass addition effects would be negligible for Mars due to the low heating environment and therefore could be eliminated.

References

[1] Cassanto, J. M., "The Base Flow Phenomena Related to Planetary Entry Probe Experiments," ALDM #71-102, April 1971, Aerodynamics Lab., Re-entry and Environmental Systems Div., General Electric Co., Philadelphia, Pa.

[2] Kemp, J. H., Jr., "Telemetry Measurements of Afterbody Pressures on Free Flying Models of the Apollo Capsule at Mach Numbers from 10 to 21 in Helium and 14 in Air," TMX-1154, Oct. 1965, NASA.

[3] Kurtz, D. W. and Kerr, W. R., "Base Pressure Distribution of Two Blunted Cones at Mach Numbers from 0.3 to 0.8 and 1.81 to 3.51," Tech. Memo. 33-403, Oct. 1968, Jet Propulsion Lab., Pasadena, Calif.

[4] Cassanto, J. M., George, F. C., and Thomas, K. M., "Recent Shock Tunnel Base Pressure Results and Application to Planetary Entry Atmospheric Probe Experiments," TIS 71 SD203, Jan. 1971, Re-entry and Environmental Systems Div., General Electric Co., Philadelphia, Pa.

[5] Cassanto, J. M. and Buce, P., "Free Fall Drop Tests to Determine Low Speed Stability and Base Pressure Characteristics on Blunt Planetary Entry Bodies," TIS 70SD294, May 1969, Re-entry and Environmental Systems Division, General Electric Co., Philadelphia, Pa.; also *Journal of Spacecraft and Rockets*, Vol. 6, No. 5, May 1969, pp. 636–637.

[6] Campbell, J. F. and Howell, D. T., "Supersonic Aerodynamics of Large-Angle Cones," TND-4719, Aug. 1968, NASA.

[7] Robinson, R. C. and Gambucci, B. J., "Fluctuating Pressures on the Afterbodies of Five Blunt Atmosphere Entry Probes," TND-4591, May 1968, NASA.

[8] Sommer, S., Boissevain, A., Yee, L., and Hedland, R., "The Structure of an Atmosphere from On-Board Measurements of Pressure, Temperature, and Acceleration," TND-3933, 1967, NASA.

[9] Sommer, S. and Yee, L., "An Experiment to Determine the Structure of a Planetary Atmosphere," *Journal of Spacecraft and Rockets*, Vol. 6, No. 6, June 1969, pp. 704–710.

[10] Cassanto, J. M., "The Effect of Bluntness Ratio and Cone Angle on Base Pressure," *AIAA Journal*, Vol. 3, No. 12, Dec. 1965, pp. 2351–2352.

[11] Whitfield, J. D. and Potter, J. L., "On Base Pressures at High Reynolds and Hypersonic Mach Numbers," AEDC TN 60-61, March 1960, Arnold Engineering Development Center, Tullahoma, Tenn.

[12] Cassanto, J. M. and Mendleson, R. S., "Local Flow Effects on Base Pressure," *AIAA Journal*, Vol. 6, No. 6, June 1968, pp. 1182–1184.

[13] Love, E. S., "Base Pressure at Supersonic Speeds on Two-Dimensional Air Foils and on Bodies of Revolution With and Without Fins Having Turbulent Boundary Layers," TN 3819, Jan. 1957, NASA.

[14] Chapman, D. R., "An Analysis of Base Pressure at Supersonic Velocities and Comparison with Experiment," Rept. 1051, 1951, NACA.

[15] Cassanto, J. M., "Base Pressure Measurements on Free Flight and Sting Supported Models at $M = 4$," *AIAA Journal*, Vol. 6, No. 7, July 1968, pp. 1411–1414.

[16] Cassanto, J. M., "Radial Base Pressure Gradients in Laminar Flow," *AIAA Journal*, Vol. 5, No. 12, Dec. 1967, pp. 2278–2279.

[17] Cassanto, J. M., and Hoyt, T. L., "Flight Results Showing the Effect of Mass Addition on Base Pressure," TIS 70 SD248, March 1970, Re-entry and Environmental Systems Division, General Electric Co., Philadelphia, Pa.; also *AIAA Journal*, Vol. 8, No. 9, Sept. 1970, pp. 1705–1707.

An Advanced Upper Atmosphere Meteorological Sounding Facility

A. A. Duff*
U.S. Army Electronics Command, White Sands Missile Range, N.Mex.

In 1960, at Fort Greely, Alaska, the author demonstrated that a remote meteorological rocket station could be operated to obtain useful wind and temperature data in the 20–65 km (66–213 kft) region on a synoptic basis using an X-band, gun-directing radar in lieu of the powerful range radars for tracking meteorological rocket payloads. Thousands of such tracks have since been obtained by various groups at Cooperative Meteorological Rocket Network (CMRN) stations throughout the world from a wide assortment of comparable tracking equipment. Continuous effort has been expended by the Atmospheric Sciences Laboratory (ASL) to optimize ground station tracking equipment at the U.S. Army stations so that maximum meteorological data can be obtained with a minimum expenditure of equipment and personnel.

A mission requirement to improve the accuracy of data obtained at Fort Greely, Alaska, and Fort Sherman, Canal Zone, and to obtain wind and density data from the surface to 105 km (334 kft) prompted the ASL to reassess the techniques and resources currently available to accomplish these objectives. As a result, advanced upper atmosphere sounding facilities are now being assembled for evaluation at the ASL, White Sands Missile Range (WSMR), New Mexico. When completed, these facilities will be transferred to the Alaskan and Canal Zone sites. Equipment and modifications to be incorporated in the advanced facilities include omnidirectional meteor trail tracking radar (MTR), a modified Nike-Hercules precision tracking radar, and a control and data handling center to integrate the meteorological data collected during operations. The MTR will obtain wind and density data in the 85–105 km (280–344 kft) altitude range, an approximate 40 km (131 kft) increase above normal rocketsonde observation altitudes. The Nike-Hercules precision radar is to be extensively modified to become a Nike-Met radar and will be used to establish calibration tables for the MTR antenna field by simultaneously tracking targets of opportunity. It will also track balloon and rocket payloads used in established sounding programs. The time-shared digital controller (Honeywell 516) will provide real-time output from the MTR, rocketsonde, rawinsonde, and pibal operations along with ballistic computations and launcher setting outputs associated with rocketsonde firings.

Meteor Trail Radar

The MTR to be fielded is a second generation, pulsed doppler model designed by ASL and incorporates certain improvements over the system previously used. The transmitting and receiving antennas are combined and consist of a radome-enclosed, all weather, mechanically stable, stacked, crossed dipole antenna with a vertical whip, centered on and located above a counterpoise. The antenna, with properly phased and amplitude controlled input through a duplexer assembly, transmits an omnidirectional, in the azimuth plane, inverted, approximately cosecant-squared pattern. In the receiving mode, again with proper phasing,

Presented as Paper 70-1392 at the AIAA 2nd Sounding Rocket Technology Conference, Williamsburg, Va., December 7–9, 1970; submitted December 9, 1970; revision received January 26, 1971.

* Senior Electronic Technician, Upper Atmospheric Research Technical Area, Atmospheric Sciences Laboratory.

the antenna and associated receivers provide multiple output voltages that, with controller processing, result in the determination of elevation and azimuth signal arrival angles. The system feeds one receiver from each of the four dipoles in the stacked cross, and the vertical whip antenna has its own receiver. It is evident that the five receivers must be closely matched in phase, gain, and gain tracking through a wide range of received signal strengths. The improved monopulse antenna system thus provides for omnidirectional operation of the MTR between elevation angles of 20° and 70° in lieu of scanning only a small volume of the surrounding atmosphere. An additional improvement provided by this system is the shaping of the transmitter rf output pulse by rf phase modulation techniques.[1] The side lobe structure of the transmitted frequency spectrum is greatly reduced, and operation in an already crowded band around 32.8 MHz is more easily accomplished with less interference. In this technique, the rf transmitter pulse is composed of two equal-amplitude and equal-shaped pulses occurring exactly in time phase. The rf phase of one of the pulses is smoothly shifted throughout its period. Thus, at the start and at the end of the pulse, its rf phase differs by 180 electrical degrees from the reference, while in the center portion of the pulse the two signals are in rf phase. The two signals are then combined in a hybrid junction to form the final transmitted pulse. A variation of this technique, where the rf phase of both pulses is changed, can produce phase-coded information within a long rf pulse.[2] This coded information can be computer processed to increase the accuracy of range determination of the meteor trail.

Digital Controller

The digital controller serves as the master synchronizer for all operations on the station, including the timing synchronization of all portions of the MTR, furnishing the master synchronizer pulse for the Nike-Met radar system, and controlling all data collection, processing, and recording functions. The controller is programed to analyze data signals and to make decisions according to a predetermined order of priority concerning the type of data collection mode in which the station should be operated. For example, a target of opportunity will prescribe a certain tracking mode. Targets of opportunity are defined as those located between ground clutter range and 85 km (279 kft), or those that persist longer than a predetermined length of time. The Nike-Met radar will then slew to this target's azimuth, elevation angle, and range and sound an alarm. When the alarm sounds, site personnel track lock the Nike-Met radar onto the target. The controller compares the very accurate track data from the Nike-Met with that from the MTR. If necessary, the controller automatically updates the antenna calibration tables of the MTR for more precise MTR observations.

Nike-Met Radar

Technical considerations and limited availability of adequate tracking radar systems led to the selection of the Nike-Hercules X-band tracking radar as the precision radar for the facility. Modifications to optimize the radar for its intended use as the Nike-Met X-band precision tracking radar include:

1) Replacement of the present antenna system with a 12-ft, fiber-glass-covered foam, Cassegrain antenna system by raising the elevation axis trunion bearings on the yoke.

2) Incorporation of a three-channel X-band parametric amplifier in the forward end of the Nike-Met radar system.

3) Mounting of a 1680 MHz monopulse antenna feed system around the X-band antenna feed for compatibility with the meteorological telemetry system (addition of this feature will permit tracking in the X-band and the 1680 MHz band simultaneously with the reception of telemetry on the 1680 MHz band antenna feed).

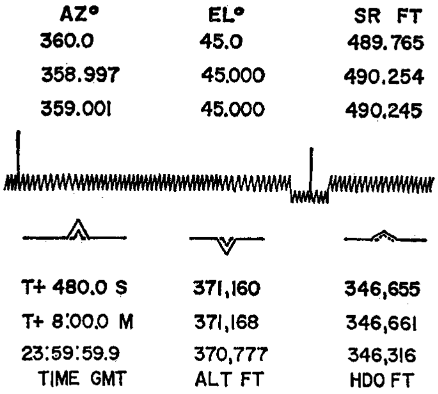

Fig. 1 Nike-Met "A" scope video display.

4) Inclusion of a parametric rf amplifier in the 1680 MHz band antenna feed system for maximum signal-to-noise ratio of the received telemetry signal.

5) Use of gray binary code plates on the azimuth and elevation axes of rotation of the antenna pedestals to encode angular data at the point of generation. Associated circuitry for data transfer to the MTR controller; encoding of range data in a 1 nsec resolution counter system for the controller.

6) Sampling of the data output from the Nike-Met radars at a 10/sec rate and recording of this information in real-time on magnetic tape.

7) Sample-and-hold and analog-to-digital conversion devices on normal video, automatic gain control, and three axes of tracking error voltages. (The information thus obtained will be combined in the digital controller with the code plate digital track information to provide more accurate total track data by the electrical elimination of mechanical tracking errors.)

8) To simplify operations, the modified system provides a display of tracking angles and other operational data of both radar pedestals on each "A" scope screen of the Nike-Met radar along with the tracking video as shown in Fig. 1. The

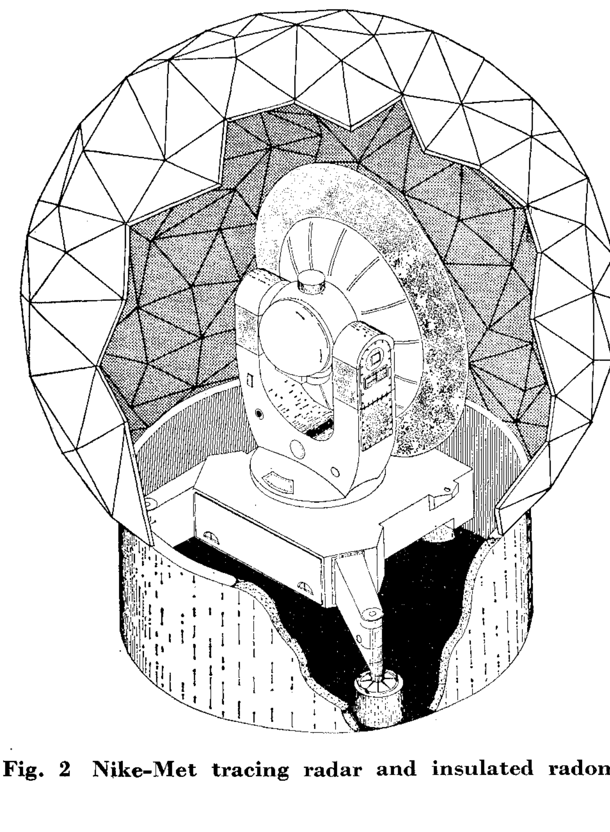

Fig. 2 Nike-Met tracing radar and insulated radome.

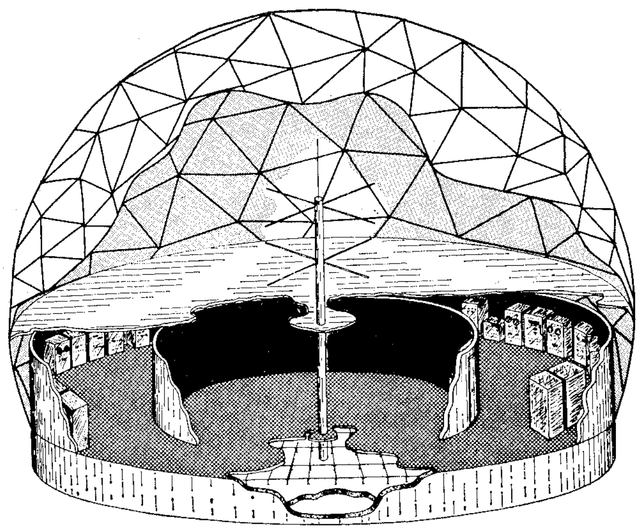

Fig. 3 Meteor trail and Nike-Met radar equipment rack layout.

last confirmed location of the target is displayed so that if the target track is lost, the operator will have the best "look" angles and range data available for reacquisition. For maximum help in acquisition, the controller can be programed prior to a rocket firing to display extrapolated look angles in real-time after the time of firing and if desired, the Nike-Met radar can be kept slewed to this extrapolated search point.

9) The Nike-Met radar is equipped with a subharmonic, pulsed transmitter and an antenna system piggy-backed and aligned with the 12-ft primary parabolic antenna with a double-the-frequency automatic frequency control (AFC) for the X-band receivers to permit the use of a two-frequency radar scheme. In this mode of operation, a pilot balloon being tracked by the radar is equipped with a 4.5 GHz harmonic generating diode in a one-half wavelength dipole wire antenna. The X-band radar transmitter is turned off, and the subharmonic transmitter emits short pulses of rf energy at 4.5 GHz. When the signal is received by the diode assembly on the balloon, it is retransmitted at twice the frequency by harmonic generation. The 9.0 GHz signal is received and tracked by the X-band Nike-Met antenna and ranging system. Since the AFC locks the receivers onto a frequency of twice the transmitter frequency, the balloon is detected at 9.0 GHz and tracked in a background free of all radar ground clutter. Tracking can occur at ranges less than those dictated by the usual recovery times of the T-R tubes (which are not used in this configuration).

The Nike-Met radar pedestals are enclosed in heated, insulated, metal space frame radomes so that all-weather maintenance and operation of the equipment can be accomplished without loss of tracking accuracy as shown in Fig. 2.

Facility Layout

The Nike-Met radar track and plot electronics racks are removed from their trailers and placed with the MTR electronics racks on a floating floor in an insulated, all dielectric radome 18 m (55 ft) in diameter as shown in Fig 3. The ceiling of the equipment room in the radome is placed at the equatorial diameter of the radome. It is made of metal faced, 4-in. polyurethane foam insulation structure board and forms the solid metal center part of the MTR counterpoise. The counterpoise, extending from the radome some 20 m (65 ft) along the radius, is composed of 15 cm (6-in.)-square electrically conducting mesh properly supported and leveled. The Nike-Met radar track pedestals in their insulated radomes are located beyond the edge of the counterpoise on a diameter through the center radome to reduce line-of-sight interference.

In areas where the sounding facility provides its own site air surveillance (such as the Alaska station) a TPS-1D surveillance radar is incorporated into the station; however, where air surveillance is provided by the range host (Fort Sherman, Canal Zone), only the MTR and the Nike-Met X-band precision tracking radars are used.

Conclusion

When installed in the summer of 1971 and completed in 1972 (funds permitting) these modified sounding facilities will provide upper atmosphere meteorological sounding support at remote sites comparable to the best missile range measurements, with a significant reduction in expenditure of material and personnel.

References

[1] Thomas, H. J. and Ward, H. P., "Study and Experimentation of RF Pulse Generating and Amplifying Techniques for Improving Radar Emission Characteristics," RD-69-33, Nov. 1969, Raytheon Co., Equipment Div., Wayland Lab.

[2] Benjamin, R., *Modulation, Resolution and Signal Processing in Radar, Sonar and Related Systems*, Pergamon Press, Oxford, 1966, p. 20.

Gravity-Induced Free Convection Effects in Melting Phenomena for Thermal Control

R. L. Bain,* F. J. Stermole,† and J. O. Golden‡
Colorado School of Mines, Golden, Colo.

Nomenclature

c_p = specific heat
d = solid-liquid interface position in y direction
k = thermal conductivity
L = length of cell in direction of long axis of cell
T = temperature
x = position in direction of long axis of cell
y = position in direction of short axis of cell, measured from the heated plate
y_0 = one-half length of cell in direction of short axis
α = angle of inclination of long axis from horizontal
ρ = density
θ = time

Subscripts

f = fusion
i = initial
l = liquid
p = hot plate
o = cold plate
s = solid

PHASE change thermal control techniques have received increasing attention, in the last several years, for spacecraft thermal design.[1-4] Because of inherent advantages of simplicity and reliability, a passive solid-liquid phase change material can be used in the walls of spacecraft as

Received January 29, 1971; revision received April 1, 1971. This work was done as a part of NASA research contract NAS8-30511, Space Sciences Laboratory, Marshall Space Flight Center, Huntsville, Ala.

* Graduate student, Chemical and Petroleum Refining Engineering Department.

† Professor, Chemical and Petroleum Refining Engineering Department.

‡ Associate Professor, Chemical and Petroleum Refining Engineering Department.